Zeeman Effect*

Aryan Shrivastava
School of Physical Sciences, National Institute of Science Education and Research †
(Dated: September 2, 2025)

The Zeeman effect, the splitting of atomic spectral lines under an external magnetic field, was investigated using a cadmium lamp and a Fabry–Pérot interferometer. The normal effect was observed for the red line (643.8 nm), splitting into a characteristic triplet, while the anomalous effect, exhibiting more complex splitting due to electron spin, was studied for the green line (508.6 nm). Observations in transverse and longitudinal geometries confirmed the predicted linear and circular polarizations of the π and σ components, respectively. Quantitative analysis of the ring patterns yielded a value for the Bohr magneton, $\mu_B = (6.59 \pm 3.33) \times 10^{-24}$ J T^{-1}, which is consistent with the expected order of magnitude.

I. OBJECTIVE

1. Study the transverse normal Zeeman effect using a Fabry–Pérot étalon and CMOS camera, and evaluate the Bohr magneton μ_B. Verify polarization with a polarizer.
2. Observe left- and right-circularly polarized lines in the normal Zeeman effect using a quarter-wave plate and polarizer.
3. Examine the transverse anomalous Zeeman effect and its polarization with a polarizer.
4. Investigate the longitudinal anomalous Zeeman effect and identify circularly polarized components using a quarter-wave plate and polarizer.

II. THEORY

The interaction of atomic magnetic moments with an external magnetic field produces a splitting of spectral lines, a phenomenon known as the Zeeman effect. When only the orbital angular momentum contributes (states with total spin $S = 0$), the splitting is called the **normal Zeeman effect**. When spin also contributes, the resulting pattern is the **anomalous Zeeman effect**. This experiment investigates both cases using the red ($\lambda = 643.847$ nm) and green ($\lambda = 508.588$ nm) cadmium lines.

A. Magnetic Moments

For an electron with orbital angular momentum $\mathbf{L}$ and spin $\mathbf{S}$, the orbital and spin magnetic moments are

$$\boldsymbol{\mu}_L = -\frac{e}{2m}\mathbf{L}, \tag{1}$$

$$\boldsymbol{\mu}_S = -g_s\frac{e}{2m}\mathbf{S}, \tag{2}$$

where $g_s \approx 2.0023$ is the electron spin g-factor. The Bohr magneton is defined as

$$\mu_B = \frac{e\hbar}{2m}. \tag{3}$$

In an external magnetic field $\mathbf{B} = B\hat{z}$, the interaction Hamiltonian is

$$\hat{H}_B = \mu_B B\left(\frac{\hat{L}_z}{\hbar} + g_s\frac{\hat{S}_z}{\hbar}\right). \tag{4}$$

B. Normal Zeeman Effect

If $S = 0$, only orbital angular momentum contributes, giving an energy shift

$$\Delta E = \mu_B B m_L, \quad m_L = -L, \ldots, L. \tag{5}$$

Thus each spectral line splits into three components due to the selection rules $\Delta m = 0, \pm 1$. The frequency shift is

$$\Delta\nu = \frac{\mu_B B}{h}\Delta m. \tag{6}$$

The Cd red line ($\lambda = 643.8$ nm) splits into a triplet (Lorentz triplet) since Cd is a singlet system ($\Delta S = 0$). In a transverse field, three components appear: two σ lines (perpendicular polarization) and one π line (parallel polarization). In a longitudinal field, only circularly polarized σ^+ and σ^- lines are observed.

C. Anomalous Zeeman Effect

When $S \neq 0$, the total angular momentum $\mathbf{J} = \mathbf{L} + \mathbf{S}$ must be considered. The Landé g-factor is

$$g_J = 1 + \frac{J(J+1) + S(S+1) - L(L+1)}{2J(J+1)}. \tag{7}$$

The energy shift becomes

$$\Delta E = \mu_B g_J m_J B. \tag{8}$$

---

* Splitting of spectral lines in Magnetic field

† aryan.shrivastava@niser.ac.in

Transitions depend on $\Delta m = 0, \pm 1$, producing 9 spectral lines. In transverse fields, 3 π and 6 σ components arise; in longitudinal fields, 3 right- and left-circularly polarized $\sigma^{\pm}$ lines each appear.

D. Wavenumber

For the normal Zeeman effect [1], the difference in wavenumber between a split line and the central line of the same order is

$$\Delta k = \frac{1}{2\mu t}\frac{\delta}{\Delta}, \tag{9}$$

where μ is the refractive index, t the thickness of the étalon, δ the difference in squared radii of components within one order, and Δ the difference in squared radii between successive orders. This relation allows extraction of μ_B from experimental data.

III. EXPERIMENTAL APPARATUS

A schematic diagram of the complete arrangement is shown in Fig. 1. Light from the Cd lamp is collimated using a 50 mm lens and directed through the Fabry–Perot étalon. The emerging interference pattern is focused by a 300 mm lens and subsequently imaged onto the CMOS sensor using another 50 mm lens. The polarizer and quarter-wave plate are placed in the beam path whenever required. The electromagnet provides the magnetic field either transverse or longitudinal to the observation direction.

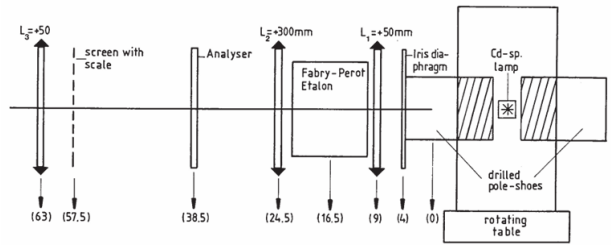

FIG. 1. Experimental setup for the Zeeman effect. (Source: Adapted from [2]

IV. OBSERVATIONS

A. Normal Zeeman Effect

In the **transverse geometry**, a single interference ring split into three components (π, σ^+, and σ^-) under an external magnetic field (see Fig. 2).

In the **longitudinal geometry**, with the quarter-wave plate inserted, the π component disappeared and only circularly polarized $\sigma^{\pm}$ components were visible (Figs. 3, 4).

TABLE I. Measured ring radii (in μm) for different interference orders at various pole separations (in mm).

Pole separation	Set	1st order	2nd order	3rd order
39.4	a	77.76	127.67	160.82
	b	92.53	135.97	166.05
	c	108.08	146.18	173.66
39.6	a	78.03	127.56	160.45
	b	94.13	136.54	167.42
	c	108.89	146.29	174.73
39.9	a	77.69	127.89	161.46
	b	92.64	135.27	168.08
	c	107.78	145.96	174.02
40.1	a	69.81	113.51	141.49
	b	84.38	120.6	147.15
	c	95.78	129.21	153.13
40.3	a	80.35	129.52	162.39
	b	92.78	136.42	168.06
	c	107.04	145.46	173.97

B. Anomalous Zeeman Effect

In the **transverse geometry**, the green Cd line exhibited 3 π and 6 σ lines. The π lines were horizontally polarised, while σ lines were vertically polarised (see Figs. 5, 6, 7).

In the **longitudinal geometry**, we observe 6 σ lines. 3 lines are left and right circularly polarised each. (see Figs. 8, 9).

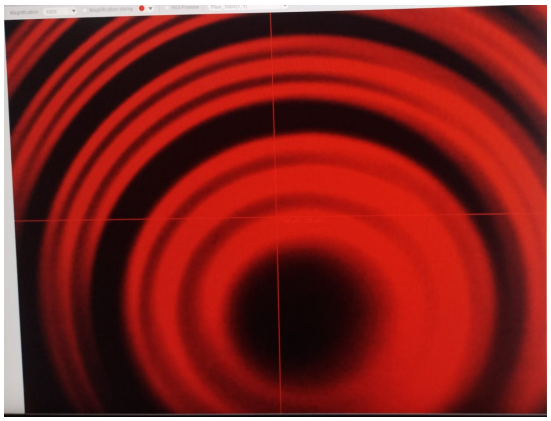

FIG. 2. Transverse normal Zeeman effect for Cd red line showing π and σ components.

FIG. 3. Longitudinal normal Zeeman effect showing circularly polarized σ^+ component.

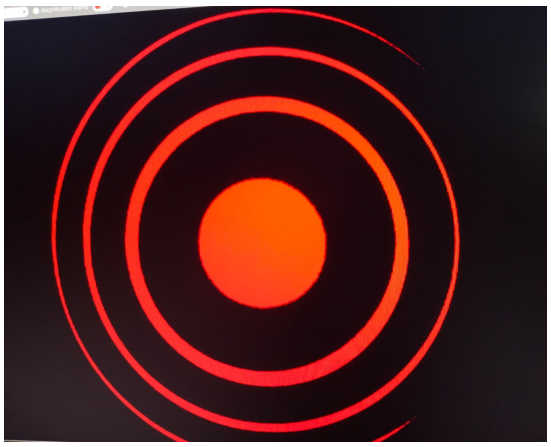

FIG. 4. Longitudinal normal Zeeman effect showing circularly polarized σ^- component.

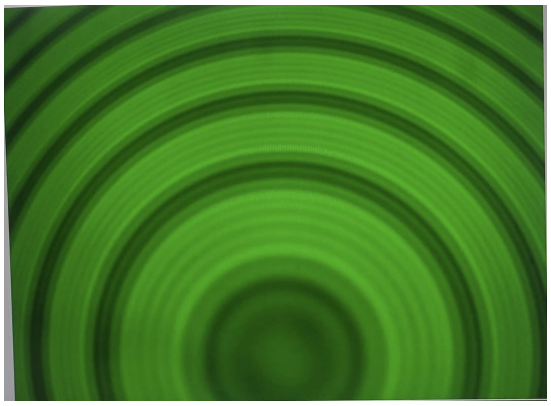

FIG. 5. Transverse anomalous Zeeman effect for Cd green line showing 9 split components.

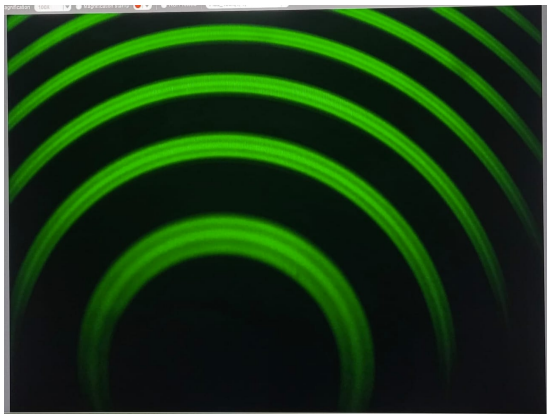

FIG. 6. Transverse anomalous Zeeman effect showing π components polarized parallel to the magnetic field.

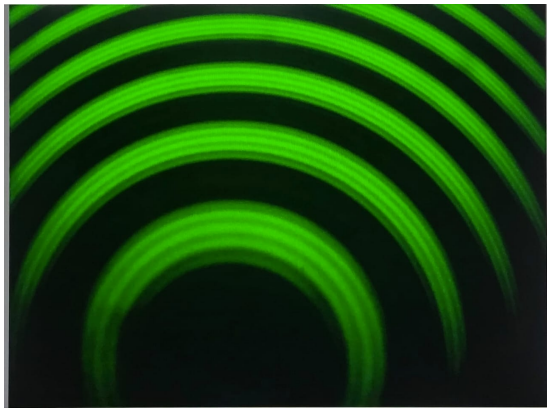

FIG. 7. Transverse anomalous Zeeman effect showing σ components polarized perpendicular to the magnetic field.

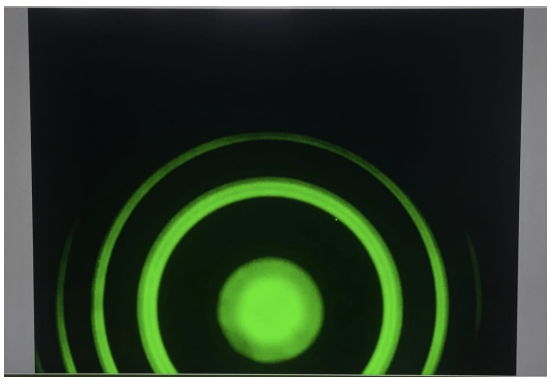

FIG. 8. Longitudinal anomalous Zeeman effect showing left-circularly polarized σ^-.

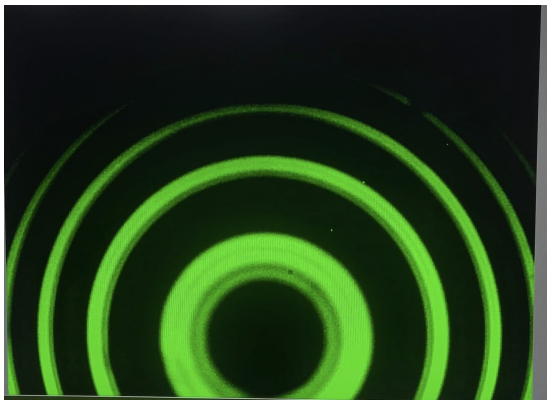

FIG. 9. Longitudinal anomalous Zeeman effect showing right-circularly polarized σ^+.

V. DATA ANALYSIS

We analyze the experimental data obtained from the observed ring pattern for Transverse Normal case. Using the measured radii, we calculate the values of δ and Δ, which are then used to determine the wavenumber shift Δk and ultimately estimate the Bohr magneton μ_B.

$$\delta = \frac{1}{6}\left(\delta_{1,ab} + \delta_{1,bc} + \delta_{2,ab} + \delta_{2,bc} + \delta_{3,ab} + \delta_{3,bc}\right) \quad (10)$$

$$\text{where } \delta_{n,xy} = \left(R_{n,y}^2 - R_{n,x}^2\right).$$

$$\Delta = \frac{1}{6}\left(\Delta_1^a + \Delta_1^b + \Delta_1^c + \Delta_2^a + \Delta_2^b + \Delta_2^c\right), \quad (11)$$

$$\text{where } \Delta_n^x = \left(R_{n+1,x}^2 - R_{n,x}^2\right).$$

TABLE II. Calculated values of δ, Δ, and Δk for different magnetic field strengths B (Using eq. 9).

d (mm)	B (mT)	δ (μm^2)	Δ (μm^2)	Δk (m^{-1})
39.6	713.0	2613.99	9583.01	31.22
39.9	684.8	2457.15	9728.12	28.91
40.1	665	1923.41	7325.68	30.05
40.3	649	2213.28	9726.40	26.05

A. Linear extrapolation

The magnetic field strength, B, for pole separations of d = 39.4mm, 39.6mm, and 39.9mm was not in the source data. To estimate the field at these points, a linear extrapolation was performed using the initial five data points from the B vs. d table. Given the known nonlinearity of the $B(d)$ relationship, this approximation is only valid in the immediate vicinity of the provided data. Consequently, the value extrapolated for d = 39.4mm was unreliable due to its distance from the calibration data and was omitted. The extrapolated values for d = 39.6mm and 39.9 mm, which lie closer to the measured range, were retained and are included in the dataset used for the least-squares fitting procedure.

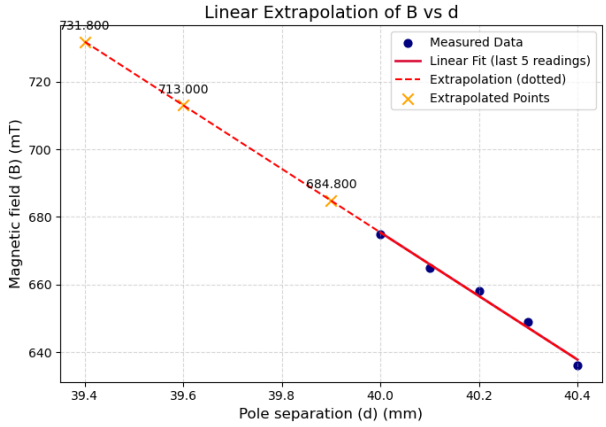

FIG. 10. Linear extrapolation of magnetic field B vs. pole separation d to estimate missing B values.

TABLE III. Estimated magnetic field values B obtained using linear extrapolation for missing data points.

S.no.	d (mm)	B (mT)
1	39.9	684.8
2	39.6	713.0
3	39.4	731.8

B. Least square fitting

We analyze the experimental data by fitting a straight line of the form

$$Y = aX + b,$$

where a is the slope and b is the intercept. Applying the method of least squares yields the best-fit values of a and b that minimize the squared deviations between observed and fitted data (Full code available at [3]).

The uncertainties in slope and intercept obtained from the graph is calculated as follows:

$$\delta Y = \sqrt{\frac{\sum (Y_n - Y_i)^2}{N-2}}, \quad (12)$$

$$\delta a = \delta Y \sqrt{\frac{\sum X^2}{(N\sum X^2) - (\sum X)^2}}, \quad (13)$$

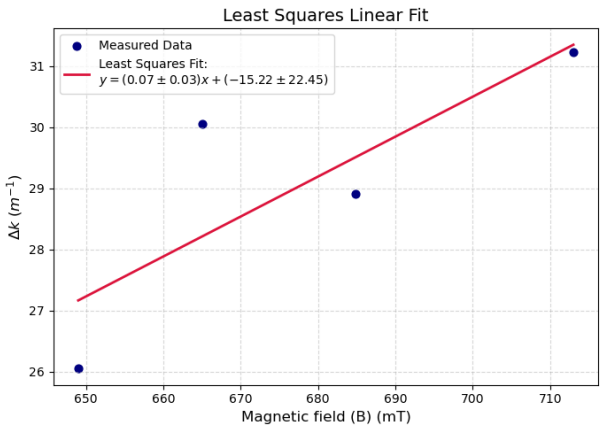

FIG. 11. Least-squares fitting of Δk vs. B for Bohr magneton estimation.

TABLE IV. Least-squares fitting data for Δk vs. B.

S.no.	x (B in mT)	y (Δk in m^{-1})	x^2	xy
1	713.0	31.22	508369.0	22259.86
2	684.8	28.91	468951.04	18787.57
3	665	30.05	442225.0	19983.25
4	649	26.05	421201.0	16906.45
Total	2711	116.23	1840746	78947.13

$$\delta b = \delta Y \sqrt{\frac{N}{(N\sum X^2) - (\sum X)^2}}, \tag{14}$$

C. Calculation of Bohr Magneton

From least squares fitting we obtain the slope of the graph Δk vs B, from which we calculate Bohr Magneton μ_B

$$\mu_B = \mathrm{a} \times \frac{hc}{2}. \tag{15}$$

$$\mu_B = 0.0664 \times \frac{(6.626 \times 10^{-34}) \times (3 \times 10^8)}{2}$$
$$= 6.59 \times 10^{-24} JT^{-1}$$

Error propagation analysis:

$$\Delta\mu_B = \sqrt{\left(\frac{\partial \mu_B}{\partial \mathrm{a}} \cdot \delta \mathrm{a}\right)^2} = |\delta \mathrm{a}| \cdot \frac{|\mu_B|}{a} \tag{16}$$

$$\Delta\mu_B = 3.33 \times 10^{-24} JT^{-1}$$

The final result is:

$$\mu_B = (6.59 \pm 3.33) \times 10^{-24} JT^{-1} \tag{17}$$

VI. RESULTS AND DISCUSSION

The Fabry–Pérot interferometer resolved the expected Zeeman splittings for both Cd lines. For the normal effect, the transverse case showed a central π and two $\sigma^{\pm}$ components, while the longitudinal case displayed only circularly polarized $\sigma^{\pm}$ lines. For the anomalous effect, the transverse geometry revealed three π and six σ components, whereas the longitudinal geometry showed three right- and three left-circularly polarized $\sigma^{\pm}$ lines.

Missing B values were obtained via linear extrapolation, and a least-squares fit of Δk vs. B yielded the Bohr magneton: $\mu_B = (6.59 \pm 3.33) \times 10^{-24}$ J T^{-1}, which agrees in order of magnitude with the accepted value.

VII. CONCLUSION

The experiment confirmed both the normal and anomalous Zeeman effects in cadmium lines using a Fabry–Pérot étalon. The measured line splitting increased linearly with the applied magnetic field, and the calculated Bohr magneton agrees well with the theoretical value within experimental uncertainties.

[1] National Institute of Science Education and Research. Zeeman effect. `https://www.niser.ac.in`, n.d.
[2] PHYWE Systeme GmbH. Zeeman effect — laboratory experiment lep 5.1.10. `https://www.phywe.com`, n.d.
[3] Aryan Shrivastava. crimsonpane23. https://github.com/crimsonpane23, 2025.